Nuclear Physics **A420** (1984) 285–296

ON THE SHAPE CONSISTENCY IN THE DEFORMED SHELL-MODEL APPROACH

J. DUDEK*, W. NAZAREWICZ** and P. OLANDERS

Department of Mathematical Physics, Lund Institute of Technology, PO Box 725, S-220 07 Lund 7, Sweden

Received 11 August 1983
(Revised 25 October 1983)

Abstract: We show that the shape inconsistency $(\beta_\lambda^V - \beta_\lambda^\varrho)$ between the average potential and the corresponding nucleonic density is generally small ($\simeq 5\%$) for $\lambda = 2, 3, 4$ in both Nilsson and Woods-Saxon models. The properties of $(\beta_\lambda^V - \beta_\lambda^\varrho)$ are analysed in detail and understood in terms of the extended Thomas-Fermi model. Approximate formulas $\beta_\lambda^\varrho = \beta_\lambda^\varrho(\beta^V)$ are given and the microscopic reasons for the shape inconsistency discussed.

1. Introduction

The aim of this paper is to examine the relation between the shape of the average shell-model potential and that of the resulting nucleonic density. For this purpose we employ both a numerical approach and the analytical, quasiclassical formulae derived by Jennings and Bhaduri [1]), and apply them to the "realistic" potentials of the Nilsson and Woods-Saxon types. In particular, we also give approximate relations between β_λ^ϱ and β_λ^V which result from our calculations †. (Here β_λ^ϱ and β_λ^V for $\lambda = 2, 3, 4, \ldots, \lambda_{\max}$ denote the quadrupole, octupole, hexadecapole ... deformations of the nucleonic density and the potential, respectively.)

We investigate in detail the microscopic reason for the inconsistencies between the two considered shapes; in particular, the contributions from (a) the Coulomb potential for protons of the Woods-Saxon model, and (b) the l^2 term of the Nilsson model are studied.

* Present address: The Niels Bohr Institutet, Blegdamsvej 17, DK-2100 København Ø, Denmark.
** On leave from Institute of Physics, Technical University, ul. Koszykowa 75, PL-00-662 Warsaw, Poland.

† Recently we learned [2]) that the dramatic differences between β_λ^ϱ and β_λ^V reported in refs. [3,4]) are incorrect and result from an error in the computer code.

2. The quasiclassical approximation for the Woods-Saxon and Nilsson densities

It is instructive to begin the discussion by recalling the quasiclassical formulae of ref. [1]) for the nucleonic density as a functional of the average potential $V \equiv V(\boldsymbol{r})$ [for a possible generalization with inclusion of a spin-orbit term, see ref. [5])]:

$$\rho(\boldsymbol{r}) = \frac{1}{3\pi^2}\left[\frac{2M}{\hbar^2}(\lambda - V(\boldsymbol{r}))\right]^{\frac{3}{2}} \times \left\{1 - \frac{1}{8}\frac{\hbar^2}{2M}\left[\frac{[\nabla V(\boldsymbol{r})]^2}{4(\lambda - V(\boldsymbol{r}))^3} + \frac{\Delta V(\boldsymbol{r})}{(\lambda - V(\boldsymbol{r}))^2}\right] + \mathrm{O}(\hbar^4)\right\} \tag{1}$$

for $(\lambda - V(\boldsymbol{r}))$ greater than zero and $\rho(\boldsymbol{r}) = 0$ otherwise. This expression is not valid near the turning point where it diverges. In eq. (1) the term in front of the curly bracket represents the standard Thomas-Fermi expression. The correction term in the curly brackets ($\sim \hbar^2$) is the semiclassical result [cf. also ref. [6]); for discussion of the $\mathrm{O}(\hbar^4)$ term see ref. [7])]. Its presence diminishes [1]) the already small discrepancies between $\rho(\boldsymbol{r})$ and the Strutinsky-smeared density [8]), $\rho_{\mathrm{S}}(\boldsymbol{r})$ defined by

$$\rho_{\mathrm{S}}(\boldsymbol{r}) \equiv \sum_{i=1}^{\infty} n_i |\psi_i(\boldsymbol{r})|^2 \tag{2}$$

(where n_i denote the Strutinsky occupation coefficients). Below we argue that the latter quantity is close to the nucleonic single-particle density

$$\rho_{\mathrm{N}}(\boldsymbol{r}) \equiv \sum_{i=1}^{A} |\psi_i(\boldsymbol{r})|^2 \tag{3}$$

which we are interested in here. Apparently the smoothing procedure represented by eq. (2) leads to the averaging over main shells and is, as a consequence, free from the local shell effects. These shell effects are displayed after introducing the so-called shell-correction to the density, $\delta\rho \equiv \rho_{\mathrm{N}} - \rho_{\mathrm{S}}$, the latter strongly related to the well known shell-correction energy δE. The geometrical shapes of the ρ_{N} and ρ_{S} densities at the nuclear surface turn out to be very similar [see fig. 1 and cf. refs. [8,9]) for an extended discussion]. Therefore eq. (1) offers some insight into the shape properties of $\rho_{\mathrm{N}}(\boldsymbol{r})$ as well.

The Woods-Saxon deformed potential used in this work is defined by

$$V(\boldsymbol{r}) = V_0/\{1 + \exp[\mathrm{dist}(\boldsymbol{r})/a]\}, \tag{4}$$

where $\mathrm{dist}(\boldsymbol{r})$ denotes the distance of the point $\boldsymbol{r}$ from the nuclear surface and a is the so-called diffuseness parameter [for more details concerning the potential and

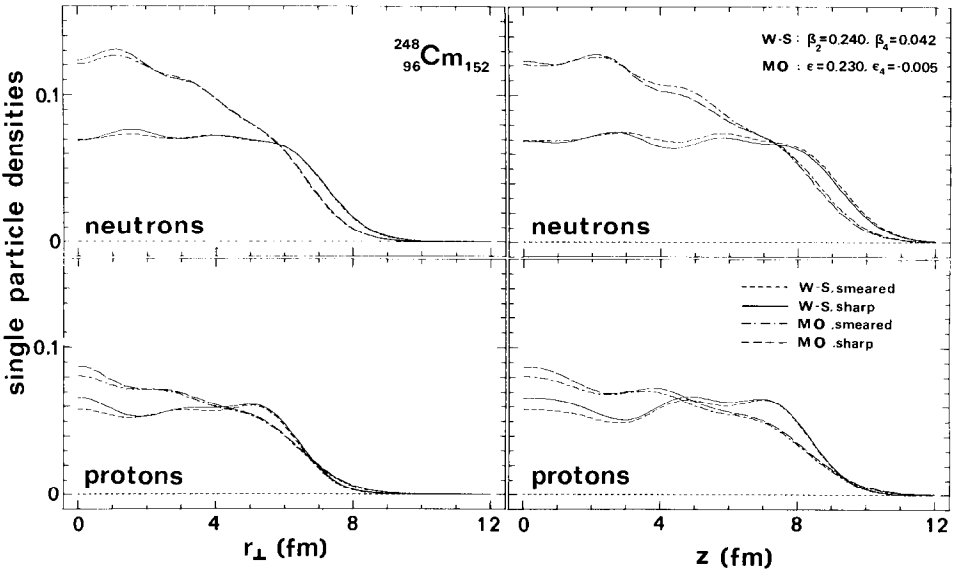

Fig. 1. Single-particle densities for the neutrons and protons (in nucleons/fm^3) of ^{248}Cm calculated in the Nilsson (MO) and Woods-Saxon (WS) models. The parameters of the Nilsson model are taken from ref. [12]) and those of the Woods-Saxon model from ref. [10]). The full and long-dashed lines correspond to the so-called "sharp" densities (eq. (3)) in the Woods-Saxon and Nilsson models, respectively. The results for the corresponding Strutinsky-smeared quantities (eq. (2)) are denoted with dashed and dash-dotted lines for the Woods-Saxon and Nilsson potentials, respectively. The cuts along the z-axis correspond to $r_\perp = (x^2+y^2)^{1/2} = 0$; those along the $r_\perp$ axis correspond to $z = 0$. The deformations correspond to the equilibrium points obtained from the Strutinsky calculations.

the numerical values of the parameters see ref. [10])]. The equation $V(\boldsymbol{r}) = \text{const}$, which defines the equipotential surfaces is strictly equivalent to the equation $\text{dist}(\boldsymbol{r}) = \text{const}$. At any surface defined by the latter we find, after simple geometrical considerations, that

$$[\nabla \text{dist}(\boldsymbol{r})]^2 = 1, \qquad \Delta \text{dist}(\boldsymbol{r}) = 0. \tag{5}$$

From eq. (5) then it follows that *on the equipotential surface* of the field (4)

$$[\nabla V(\boldsymbol{r})]^2 = \frac{V_0^2}{a^2} \frac{\exp[2\text{dist}(\boldsymbol{r})/a]}{\{1+\exp[\text{dist}(\boldsymbol{r})/a]\}^4}, \tag{6a}$$

$$\Delta V(\boldsymbol{r}) = -\frac{V_0}{a^2} \exp[\text{dist}(\boldsymbol{r})/a] \frac{1-\exp[\text{dist}(\boldsymbol{r})/a]}{\{1+\exp[\text{dist}(\boldsymbol{r})/a]\}^3}, \tag{6b}$$

and therefore the square of the gradient of the potential (6a) and the laplacian of the potential (6b) are also constant there. Inserting (6a, b) into (1) shows,

furthermore, that the Woods-Saxon equipotential surfaces are simultaneously surfaces of constant density up to $O(\hbar^4)$ in terms of the semiclassical corrections to the Thomas-Fermi formula. [Apparently the spatial variation of the potential and the corresponding density are in general different. It should also be mentioned that any two equipotential surfaces defined, say, by $V(\boldsymbol{r}) = \text{const}$ and $V(\boldsymbol{r}) = \text{const}'$, are generally *not* geometrically similar for different values of const and const'.]

The properties of the Nilsson potential are different in the respect discussed. This can easily by verified after noticing that for a pure harmonic oscillator the equation

$$V_{\text{osc}}(\boldsymbol{r}) \equiv 0.5\, m\, (\omega_x^2 x^2 + \omega_y^2 y^2 + \omega_z^2 z^2) = \text{const} \tag{7a}$$

does not imply that

$$[\nabla V(\boldsymbol{r})]^2 = m\, (\omega_x^4 x^2 + \omega_y^4 y^2 + \omega_z^4 z^2) \tag{7b}$$

is constant although

$$\Delta V_{\text{osc}}(\boldsymbol{r}) = m\, (\omega_x^2 + \omega_y^2 + \omega_z^2) \tag{7c}$$

is trivially constant no matter which equipotential surface is considered. Consequently one may expect that the shape inconsistency ($\beta^V \neq \beta^\rho$) may be of some importance in the Strutinsky calculations for the harmonic oscillator or Nilsson-model potentials (in the case of the Nilsson potential the eqs. (1), (7a–c) become more complex due to terms containing the (stretched) angular momentum $\boldsymbol{l}_t$ and higher-order deformations), but it is most likely negligible at least for a pure Woods-Saxon well. Here it should be emphasized, however, that the geometrical considerations expressed by (5)–(6) can in general not be repeated for the Coulomb potential added to the proton Woods-Saxon potential and thus the proton and neutron shape-consistency conditions are expected to be quite different there. On the contrary, due to similar mathematical forms of the proton and neutron Nilsson-model potentials the discrepancies $\beta_\lambda^\rho - \beta_\lambda^V$ should be similar for both kinds of particles in this case.

The effective potential obtained by adding the Coulomb and the Woods-Saxon terms for protons has equipotential surfaces which, in general, differ from those characteristic for the Woods-Saxon term alone. Therefore, by assuming common values of β_λ^V for both protons and neutrons we allow for different geometries of the two kinds of particles. Alternatively, one could redefine the proton potential by assuming that, for instance, the geometry of either the equipotential or equidensity surfaces are identical at the nuclear surface for both kinds of particles. We feel, however, no strong physical motivation for the latter alternative since the proton and the neutron densities do manifest different spatial behaviour as has been confirmed experimentally. Thus in the following we do not distinguish between the

proton and the neutron *potential* deformations in neither of the two potentials discussed. Further consequences of the Coulomb repulsion on the shape inconsistency are illustrated in sect. 3.

It is worth emphasizing that the inaccuracies of the Thomas-Fermi and extended Thomas-Fermi approximations connected with the turning-point problem do not influence the validity of this discussion. The *geometrical* arguments above are valid, of course, for considered surfaces inside the surface $V(\boldsymbol{r}) = \lambda$. The latter "turning-point" surface corresponds to the tail region of the quasiclassical density [see refs. [1,7,11])] and in the "half-density" region we have $V(\boldsymbol{r}) < \lambda$. Moreover, all the quasiclassical multipole moments defining the nuclear shape can be obtained by simple integration of (1) using the method described in refs. [1,7,11]).

3. Results and discussion

The considerations presented in sect. 2 are fully confirmed by our numerical calculations. Results which depend on deformation are represented below with the help of the so-called β-parametrization for both the Nilsson and Woods-Saxon potentials. This parametrization is introduced by

$$R(\theta) = c(\beta)R_0\left[1 + \sum_{\lambda} \beta_\lambda Y_{\lambda 0}(\cos\theta)\right], \qquad R_0 = r_0 A^{\frac{1}{3}}, \tag{8}$$

where $\beta \equiv \{\beta_2, \beta_3, \ldots\}$ and $c(\beta)$ is calculated from the constant volume condition. Since the Nilsson model is traditionally parametrized in terms of the so-called ε-parametrization [cf. ref. [12]) for details and potential parameter values], a transformation between the two parametrizations is needed when comparing the results of the two approaches. This transformation is done by requiring that for a given set of parameters (either β or ε) the other set (either ε or β) fulfills the condition

$$\frac{Q_\lambda^{\text{macro}}(\varepsilon)}{Q_0^{\text{macro}}(\varepsilon)} = \frac{Q_\lambda^{\text{macro}}(\beta)}{Q_0^{\text{macro}}(\beta)}, \qquad \lambda = 2, 3, 4 \ldots \lambda_{\max}, \tag{9}$$

with $\lambda_{\max}$ chosen in such a way that the transformation result does not depend on its particular value [9]). [Let us also mention that in order to transform shapes defined by, say, given ε_2 and ε_4, generally a larger number of β parameters (e.g. β_2, β_4, β_6 and β_8) different from zero is involved. For the deformations considered in this paper it was sufficient to set $\lambda_{\max} = 10$.] The "surface" multipoles in eq. (9) are defined [according to ref. [3])] by

$$Q_\lambda^{\text{macro}} \equiv \int \mathrm{d}^3\boldsymbol{r}\rho_{\text{un}}(\boldsymbol{r})r^2 Y_{\lambda 0}(\Omega), \tag{10}$$

while the "uniform" density distribution is

$$\rho_{\mathrm{un}}(\boldsymbol{r}) \equiv \begin{cases} \rho_0 \text{ for } \boldsymbol{r} \text{ inside the surface } \Sigma \\ 0 \text{ otherwise} \end{cases} \tag{11}$$

(here Σ denotes the surface defined in eq. (8)). The normalisation (9) makes the transformation independent of the details of the volume conservation condition as well as the particular values of the uniform-density radius parameter (both irrelevant when comparing geometrical shapes).

In the following we refer to the quantity $(\beta^V - \beta^\rho)$ as the *shape inconsistency*. In order to calculate this quantity from, say, a given density $\rho_{\mathrm{S}}(\boldsymbol{r})$ another transformation is necessary. For this purpose we first calculate the so-called microscopic surface moments

$$Q_\lambda^{\mathrm{micro}} = \int \mathrm{d}^3\boldsymbol{r}\rho_{\mathrm{S}}(\boldsymbol{r})r^2 Y_{\lambda 0}(\Omega), \tag{12}$$

and then we determine the corresponding β^ρ after modifying condition (9) to

$$\frac{Q_\lambda^{\mathrm{macro}}(\beta^\rho)}{Q_0^{\mathrm{macro}}(\beta^\rho)} = \frac{Q_\lambda^{\mathrm{micro}}(\beta^V)}{Q_0^{\mathrm{micro}}(\beta^V)}, \qquad \lambda = 2, 3, 4 \ldots \lambda_{\max} \tag{13}$$

(see also the discussion above).

The calculated single-particle densities corresponding to the Strutinsky-smeared (eq. (2)) and the "sharp" (eq. (3)) nucleonic distributions are shown in fig. 1 for ^{248}Cm as an illustrative example of a heavy nucleus. The figure shows, in addition to the well-known [8]) differences between the spatial density distributions of the Nilsson and Woods-Saxon models, that $\rho_{\mathrm{S}}(\boldsymbol{r})$ and $\rho_{\mathrm{N}}(\boldsymbol{r})$ are very close to each other (for a given potential and kind of particles) especially at the nuclear surface. Such information is useful when examining qualitatively the properties of $\rho_{\mathrm{N}}(\boldsymbol{r})$ with the help of (1).

Fig. 2 illustrates the shape inconsistency for quadrupole ($\lambda = 2$, top) and hexadecapole ($\lambda = 4$, bottom) degrees of freedom as a function of β_2^V. As expected, the proton and neutron shape inconsistencies are nearly identical in the case of the Nilsson model but quite distinct in the Woods-Saxon case. The repulsive character of the Coulomb potential manifests itself characteristically in the negative values of $(\beta_2^V - \beta_2^\varrho)$ for elongations ($\beta_2 > 0$) and positive values for oblate shapes ($\beta_2 < 0$). Similarly, the negative values of the hexadecapole shape inconsistency $(\beta_4^V - \beta_4^\varrho)$ can be understood as a tendency to repel protons to the most "remote"areas of space available within a given nuclear shape. The curves in fig. 2 correspond to $Z = 68$ and $N = 100$ (^{168}Er nucleus). However, in order to demonstrate that the figure represents a typical behaviour and that the results discussed do not depend very

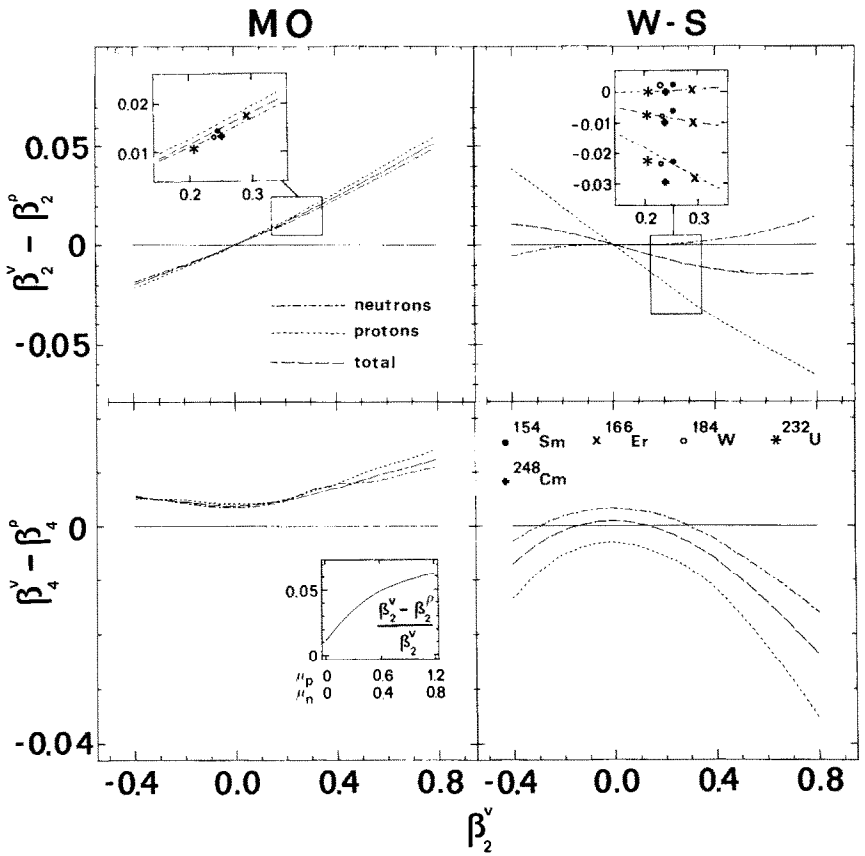

Fig. 2. The quadrupole shape inconsistencies $(\beta_2^V - \beta_2^\rho)$ (top) and the hexadecapole shape inconsistencies $(\beta_4^V - \beta_4^\rho)$ (bottom) for the Nilsson (MO) and Woods-Saxon (WS) models as function of the quadrupole deformation β_2^V (the hexadecapole deformation is fixed: $\beta_4^V = 0.05$). The lines correspond to the calculations for the ^{168}Er nucleus but they are representative for the general trends in shape inconsistencies of medium-heavy and heavy nuclei as indicated by the results for ^{154}Sm, ^{166}Er, ^{184}W, ^{232}U and ^{248}Cm nuclei. [Nilsson model results refer to the total (sum of the proton and the neutron contributions) shape inconsistencies.] The latter correspond to the equilibrium deformations of the indicated nuclei (insets in the uper part). Inset in the bottom-left part of the figure shows the typical total quadrupole shape inconsistency as a function of the μ-parameter (the strength parameter of the l_t^2 term in the Nilsson model); corresponding results indicate that bulk of the shape inconsistency there is due to the l_t^2 term.

much on either the particular nucleus selected or its equilibrium deformation, the calculations were repeated for a few nuclei whose equilibrium deformations are known to be very different (^{154}Sm, ^{166}Er, ^{184}W, ^{232}U and ^{248}Cm). The results of fig. 2 (insets, top part) show the generality of the discussed geometrical trends and confirm earlier results [13,14]. [Note that in refs. [13,14]) the standard definition of multipole moments (i.e. $Q_{\lambda 0} \sim \langle r^\lambda Y_{\lambda 0} \rangle$) has been used. This made the volume

effects more important in these results as compared to the results in this paper, where the "surface" moments (i.e. $Q_{\lambda 0} \sim \langle r^2 Y_{\lambda 0} \rangle$, cf. eqs. (10), (12)) are used.]

The calculations show also that the bulk of the shape inconsistency in the Nilsson model originates from the l_t^2 term in the potential; when varying the corresponding μ-parameters from 0 up to their "realistic" values ($\mu_p \simeq 0.6$ and $\mu_n \simeq 0.4$), the shape inconsistency ($\beta_4^V - \beta_4^\rho$) increases from $\sim 1\%$ to $\sim 6\%$ as is illustrated in the bottom part of the figure (inset). These results also indicate that the spin-orbit term contributes much less to the shape inconsistency [in the case of the Woods-Saxon potential a very small spin-orbit effect on the shape inconsistency is caused by the difference in the nuclear surface radii r_0 (see eq. (8)) of the central and spin-orbit parts which influences the actual dist(r) value; for details of the spin-orbit potential parametrisation, cf. ref. [10])].

Fig. 3 illustrates all the relations discussed in connection with fig. 2, but as a

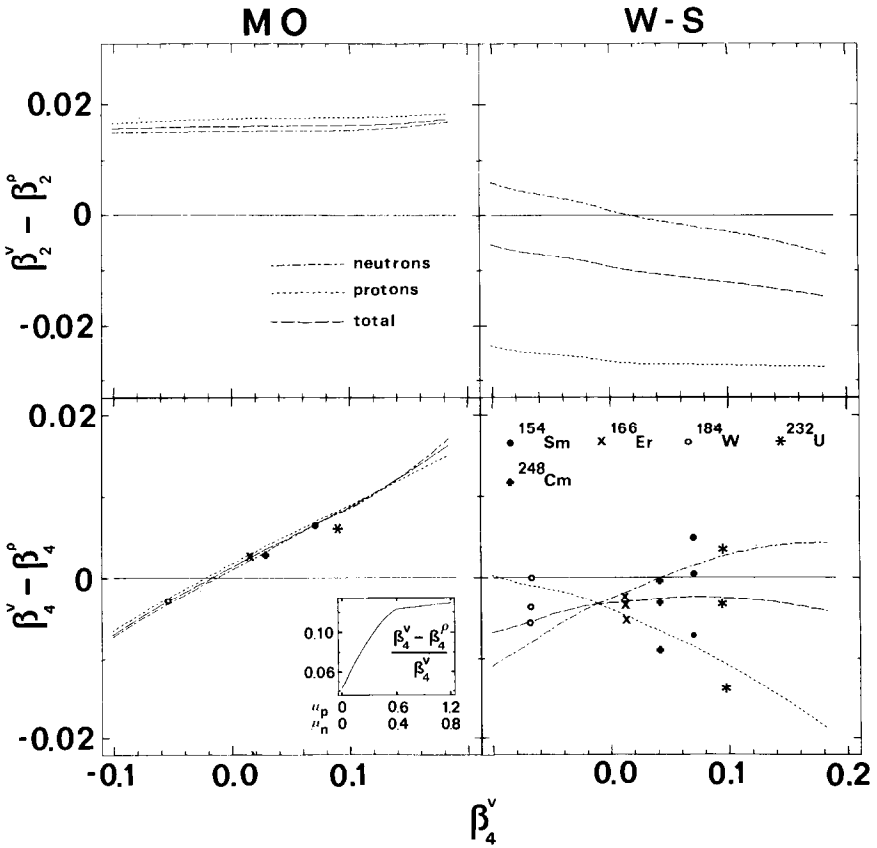

Fig. 3. Analogous to fig. 2 but showing the deformation dependencies in function of the hexadecapole deformation β_4^V. The quadrupole deformation is fixed: $\beta_2^V = 0.275$.

function of the hexadecapole deformation. By comparing the two figures one learns that in the Nilsson model the quadrupole shape inconsistency is nearly independent of β_4^V and the hexadecapole shape inconsistency nearly independent of β_2^V for both neutrons and protons. In the Woods-Saxon case the neutron shape inconsistencies are generally negligible, and amount only in the case of $\lambda = 4$ to ~ 0.015 at $\beta_2 = 0.8$ (!). However, the proton shape inconsistencies are generally at least of a factor of 2 larger, and often of the opposite sign, as compared to those of the neutrons. All these effects can be understood in terms of the generalized Thomas-Fermi formula (1) after taking into account the repulsive character of the Coulomb interaction, as stressed in the discussion above.

One of the interesting applications of the above geometrical considerations has been proposed [3]; it consisted in generalizing the shell-correction method of Strutinsky [15]) by imposing the so-called shape-consistency condition. The main idea of the Strutinsky method consists in approximating the expression for the total nuclear energy by the sum of the so-called macroscopic (usually a classical liquid drop or alternatively a droplet model) and the quantal, microscopic (the so-called shell-correction) terms. The microscopic part can be expressed explicitly [8,12,15,16]) in terms of the single-particle energies of the deformed shell model and thus depends clearly on the *potential* deformation parameters β_λ^V. The macroscopic part describes the bulk properties of the *nuclear matter distribution* in the nucleus, and should in fact depend on the deformation parameters β_λ^ρ of the latter, as proposed by Nerlo-Pomorska and Pomorski [3]). The improved Strutinsky formula reads

$$E_{\text{total}} = E_{\text{macro}}[\beta^\rho(\beta^V)] + \delta E_{\text{micro}}(\beta^V). \tag{14}$$

This form of the Strutinsky formula stresses the fact that the potential deformation β^V plays an auxiliary role while the "physical" shape is that associated with β^ρ (nucleonic density). Eq. (14) constitutes a mathematical expression of the so-called shape-consistency (or simple-consistency) condition in the shell-correction method.

Our results which show that shape inconsistencies are generally small, even at very large nuclear elongations, differ markedly from the results of refs. [3,4]) (cf. footnote above). This is also valid for pear-shaped deformations as illustrated in fig. 4; the octupole shape inconsistencies are quite small in both Nilsson and Woods-Saxon models and do not generally exceed $\sim 5\%$ for the total (i.e. neutron + proton) densities [in contrast to the results of refs. [4,17]) where about 50% differences between β_3^ρ and β_3^V are reported]. Therefore the shape-consistency condition cannot help much in explaining e.g. stable octupole deformations in some actinides [see also discussion in ref. [18])].

By analysing the results for a number of nuclei in the rare-earth and actinide regions we have found the following simple parametrizations approximating the calculated shape inconsistencies:

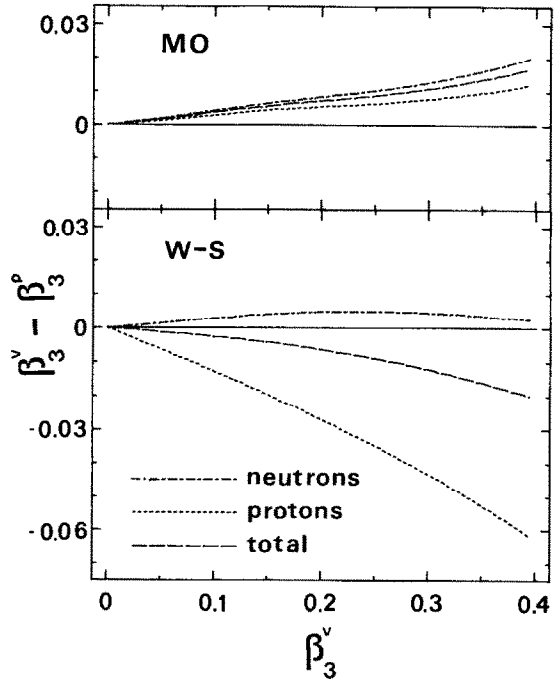

Fig. 4. The octupole shape inconsistencies $(\beta_3^V - \beta_3^\rho)$ as functions of the octupole degree of freedom β_3^V calculated for ^{222}Ra. The other β_λ degrees of freedom varying there (not displayed) correspond to the "shape trajectory" $\varepsilon_2 = 0.2$, $\varepsilon_4 = -0.04$, $\varepsilon_3 = (0\text{–}0.30)$, $\varepsilon_5 = -0.9\ \varepsilon_2\varepsilon_3$; for the choice of this particular trajectory, cf. ref. [18]).

(*a*) *Nilsson model*:

$$\beta_2^\rho \simeq 0.95\ \beta_2^V(1-0.01\ \beta_2^V) \tag{15a}$$

valid for $-0.1 < \beta_4^V < 0.2$ and nearly independent of β_4^V;

$$\beta_4^V \simeq 0.91\ \beta_4^V - 0.01\ (\beta_2^V)^2 \tag{15b}$$

valid for $-0.4 < \beta_2^V < 0.8$ and $0.1 < \beta_4^V < 0.2$;

$$\beta_3^\rho \simeq 0.96\ \beta_3^V \tag{15c}$$

valid, on the average, in the (β_2^V, β_4^V) regions corresponding to the ground-state equilibrium deformations of actinide (or rare-earth) nuclei.

All the above relations are valid simultaneously for the neutron and proton shape inconsistencies.

(*b*) *Woods-Saxon model*:

$$\beta_2^\varrho \simeq \begin{cases} 1.10\,\beta_2^V - 0.03\,(\beta_2^V)^3, & \text{protons} \quad (16a) \\ \beta_2^V - 0.04\,(\beta_2^V)^3, & \text{neutrons}, \quad (16b) \end{cases}$$

valid for $-0.1 < \beta_4^V < 0.2$ and almost independent of β_4^V;

$$\beta_3^\varrho \simeq \begin{cases} 1.15\,\beta_3^V, & \text{protons} \quad (16c) \\ \beta_3^V, & \text{neutrons}, \quad (16d) \end{cases}$$

valid for β_2 and β_4 in the vicinity of the ground-state equilibrium deformations of the actinide nuclei.

4. Conclusions

The systematic differences between shapes of the deformed shell-model potentials and the corresponding shapes of the nucleonic densities have been studied using both Nilsson and Woods-Saxon models. The general properties of the shape inconsistency (defined as $(\beta_\lambda^V - \beta_\lambda^\varrho)$) have been discussed in terms of the extended Thomas-Fermi model; they are confirmed by the numerical calculations performed for a number of nuclei from the rare-earth and actinide regions. We find that the proton and neutron shape inconsistencies are very similar for the Nilsson model, but very distinct for the Woods-Saxon model. In particular, the charge distributions are more deformed than the mass distributions in the Woods-Saxon calculations, while they are almost the same in the Nilsson calculations. This fact may be important when interpreting the results of measurements of the charge multipole moments in terms of the total (mass) multipole moments with the help of either of the two potentials.

The absolute values of the shape inconsistencies are found to be small (usually not exceeding 5% of the actual deformation value) not only in the vicinity of the equilibrium point, but in the whole considered deformation range [see also the discussion in ref. [8])]. Therefore we conclude that the so-called shape-consistency condition [3]) in the Strutinsky formula does not lead to any significant modifications of results of the "traditional" Strutinsky method.

We are grateful to I. Ragnarsson for continous interest, discussions and suggestions; helpful discussions with T. Berggren are also acknowledged. J. D. would like to acknowledge support from the Danish Research Council during his stay at the NBI. W.N. gratefully acknowledges the support from the Swedish Natural Research Council (NFR) in the form of a postdoctoral fellowship in Lund.

References

1) B. K. Jennings and R. K. Bhaduri, Nucl. Phys. **A237** (1975) 149
2) K. Pomorski, 1983, private communication
3) B. Nerlo-Pomorska and K. Pomorski, Nukleonika **22** (1977) 289
4) B. Nerlo-Pomorska, Nukleonika **23** (1978) 119; Nucl. Phys. **A327** (1979) 1; Z. Phys. **A293** (1979) 9;
   B. Nerlo-Pomorska and K. Pomorski, Z. Phys. **A309** (1983) 341;
   P. Rozmej, B. Nerlo-Pomorska and K. Pomorski, Nucl. Phys. **A405** (1983) 252
5) B. K. Jennings, R. K. Bhaduri and M. Brack, Nucl. Phys. **A253** (1978) 29
6) R. Balian and C. Bloch, Ann. of Phys. **63** (1971) 592;
   P. Ring and P. Schuck, in The nuclear many-body problem, (Springer, New York, 1980) p. 537
7) B. K. Jennings, Ph.D. thesis, University of McMaster 1976)
8) M. Brack, J. Damgaard, H. C. Pauli, A. S. Jensen, V. M. Strutinsky and C. Y. Wong, Rev. Mod. Phys. **44** (1972) 320
9) R. Bengtsson, J. Dudek, W. Nazarewicz and P. Olanders, to be published
10) J. Dudek, Z. Szymański and T. Werner, Phys. Rev. **C23** (1981) 920
11) O. Bohigas, X. Campi, H. Krivine and J. Treiner, Phys. Lett. **64** (1976) 381
12) S. G. Nilsson, C.-F. Tsang, A. Sobiczewski, Z. Szymański, S. Wycech, C. Gustafson, I. L. Lamm, P. Möller and B. Nilsson, Nucl. Phys. **A131** (1969) 1
13) J. Dudek, W. Nazarewicz and P. Rozmej, Nukleonika **25** (1980) 1049; J. of Phys. **G6** (1980) 1521; W. Nazarewicz and P. Rozmej, Nucl. Phys. **A369** (1981) 36
14) P. Olanders, graduation thesis (1977)
15) V. M. Strutinsky, Nucl. Phys. **A95** (1967) 4
16) M. Bolsterli, E. O. Fiset, J. R. Nix and J. R. Norton, Phys. Rev. **C5** (1972) 1050;
   S. Bjørnholm and J. E. Lynn, Rev. Mod. Phys. **52** (1980) 725
17) A. Gyurkovich, A. Sobiczewski, B. Nerlo-Pomorska and K. Pomorski, Phys. Lett. **105B** (1981) 95
18) G. A. Leander, R. K. Sheline, P. Möller, P. Olanders, I. Ragnarsson and J. A. Sierk, Nucl. Phys. **A388** (1982) 452